EAI Endorsed Transactions
on Energy Web
Research Article EAI.EU

Research on Optimization of Flexibility Resources for Urban Power Grids Considering Energy Storage Devices and Industrial Load Power Regulation

Yucheng Ding*, Guanglong Xie and Xiaoling Jin

State Grid Energy Research Institute, Beijing 102209, China

Abstract

Faced with the challenges of uncertainty and volatility in power output brought by high-penetration new energy integration, traditional regulation resources struggle to independently support the stable operation of urban power grids, making it urgent to establish an effective optimization mechanism for flexible resource allocation. To this end, this paper aims to investigate the synergistic planning of energy storage systems and industrially adjustable loads to enhance the resilience, security, and economic efficiency of urban power grids. To achieve this objective, a bi-level optimization model based on long- and short-term time scale coupling is constructed: the outer-level model focuses on ensuring secure grid operation under extreme scenarios such as N-1 contingencies, determining the minimum required capacity of energy storage and adjustable loads at each node through multi-contingency power flow analysis, thereby establishing a rigid safety boundary for the system. Building upon this, the inner-level model aims for optimal economic performance in typical daily operation, comprehensively considering new energy fluctuations, load characteristics, and regulation costs. It dynamically optimizes energy storage charging/discharging strategies, industrial load regulation pathways, and necessary resource expansion plans, while incorporating wind and solar curtailment variables to enhance model adaptability. Through iterative solving between the two levels, the model achieves an organic integration of safety boundaries from the planning phase with economic dispatch in the operational phase.Case study results based on a six-node system demonstrate that the proposed model can provide differentiated energy storage configurations and load retrofit schemes for various scenarios such as real-time control, peak shaving, and valley filling, effectively leveraging the differences in load characteristics among nodes. A comparative study shows that, under the premise of meeting the same flexibility requirements, the synergistic "storage-load" configuration scheme can effectively reduce both the scale of energy storage investment and the total system cost (by approximately 7.3%) compared to a single-mode approach relying solely on storage, and also helps reduce new energy curtailment losses. This research confirms the effectiveness of the constructed bi-level optimization model in coordinating safety and economic objectives and promoting complementary synergy among diverse resources. It provides a theoretically sound and practically guiding methodology and decision-making support for flexible resource planning in urban power grids under high-penetration new energy integration.

Keywords: City power grid, Flexible resource optimization, Energy storage equipment, Industrial load power regulation, Bilevel programming model

Received on 01 October 2025, accepted on 21 December 2025, published on 15 April 2026

doi: 10.4108/ew.12142

1. Introduction

With the continuous increase in renewable energy installation capacity and the steady advancement of the "dual carbon" goals, the operation mode of the power system is undergoing

*Corresponding author. Email: 675281777@qq.com

a profound transformation from centralized to distributed, and from rigid control to flexible regulation [1-2]. The high-penetration integration of renewable energy sources such as wind and solar power has introduced new challenges, including strong uncertainty and high volatility in their output [3-4]. Traditional regulation resources (such as thermal and hydro power) struggle to independently support the stable operation of the system. Therefore, as a critical link that hosts a large number of distributed energy resources and energy consumption terminals, urban power grids urgently need to establish an optimal allocation mechanism for flexible resources to enhance their self-adaptive capability in accommodating renewable energy and responding to operational disturbances.

In the urban load structure, industrial load constitutes a significant proportion, particularly industrial processes with regulatory potential (such as aluminium electrolysis, steelmaking, electric furnace loads, etc.), which possess inherent response capabilities. Meanwhile, energy storage systems (e.g., lithium-ion batteries, flow batteries, etc.) serve as regulating buffers between "source and load," demonstrating unique advantages in achieving peak shaving and valley filling, providing backup substitution, and responding to load variations [5-6]. Therefore, investigating the flexible resource allocation of grid in the coordination of industrial load regulation and energy storage systems has important theoretical and practical significance for enhancing the resilience, security, and economy of urban grid operation.

With the high-penetration integration of distributed renewable energy, the volatility and randomness of its output pose severe challenges to the economical and stable operation of the power system. To address these challenges, the academic community has conducted research on the optimal dispatch of flexible resources from various perspectives. Regarding dispatch strategies, some studies have proposed a two-stage optimized intraday dispatch strategy for demand-side flexible resources to directly counteract the impact of renewable energy fluctuations [7]. Other research has focused on assessing the response potential of user-side flexible resources [8], quantifying their support capabilities for grid planning and operation by simulating optimal operation sequences. In terms of control and optimization methods, some work has concentrated on the optimal combined control of demand response resources [9], utilizing the active response of flexible loads to eliminate equipment overloading issues. Other studies have developed distributed resource optimization configuration methods based on intelligent algorithms [10], aiming to meet system reliability requirements at the lowest cost. Furthermore, some literature has systematically categorized demand-side resource types and interaction strategies to ensure grid security and stability [11]. In the frontier of technology, artificial intelligence methods such as graph neural networks and attention mechanisms have been introduced for load forecasting, improving model accuracy and robustness [12]. Simultaneously, for renewable energy accommodation, multi-type demand response collaborative optimization models and dynamic support models for specific equipment like PEM fuel cells have also been developed [13-14]. Notably, existing research has proposed a novel flexible load scheduling architecture for urban power grids [15], enhancing grid dispatch flexibility from the load side. Overall, existing research has achieved substantial results in load-side resource scheduling, response potential assessment, and collaborative control, laying a foundation for improving grid flexibility.

Furthermore, current research on flexible resource planning predominantly focuses on single regulation entities, lacking a multivariate coordination modelling framework. Moreover, there is often a disconnect in the temporal dimension between the planning phase and the operational phase, leading to suboptimal performance of resource allocation schemes in practice.

Meanwhile, the power regulation capability of industrial loads is closely tied to the physical characteristics and control logic of their production processes, resulting in a certain delay in their response to grid dispatch instructions. This delay primarily stems from two levels: first, the communication and control system delay for signal reception, processing, and command issuance, typically ranging from seconds to minutes; second, the adjustment time required for the physical state of the load equipment itself, such as the start-stop of large motors, power ramping of electric heating furnaces, or current regulation of electrolytic cells, which depends on equipment inertia and process constraints, with delay times varying from tens of seconds to several tens of minutes. Specifically, loads like aluminum electrolysis and electric arc furnaces can achieve power changes within seconds to minutes by rapidly adjusting current, whereas continuous production processes such as steel rolling and cement calcination often require power regulation to align with production rhythms and safety protocols, leading to response delays that may range from several minutes to over ten minutes.

Therefore, this paper centers on "load-storage" synergy and integrates multi-time scale optimization theory to explore operable and implementable methods for flexible resource allocation. This study is instrumental in advancing the construction of new-type power systems in urban grids, supporting the high-penetration integration of distributed energy resources, and facilitating load-side participation in system optimization and regulation.

The essence of flexible resource planning in urban power grids lies in addressing the optimal allocation of different types of regulating resources across multiple spatial and temporal levels. When considering the synergy between industrial load power regulation and energy storage systems, the model design must simultaneously address the following challenges First, the coordinated modelling of multiple types of regulating entities is complex. Industrial load regulation is characterized by strong constraints and process coupling, influenced by factors such as production lines and equipment operating states, making it less flexible to control compared to controllable power sources. Meanwhile, energy storage systems are subject to physical constraints such as charge/discharge power capacity, energy limits, and lifecycle costs [16]. Coupling and optimizing both in a unified model requires accurately representing the characteristics of different resources while reflecting their synergistic

capabilities at the system level, which presents significant modelling difficulties. Second, the impact of spatial layout on system operation has not been effectively characterized [17-18]. The deployment of flexible resources at different locations in the distribution network significantly affects power flow, voltage support, and regulation efficiency. Traditional models often simplify or neglect the influence of deployment locations, leading to issues such as low regulation efficiency and response failures in later operational stages. Therefore, it is necessary to introduce network feasibility constraints into the planning model, enabling the coupling of resource layout with system topology and electrical parameters for comprehensive optimization. Third, cross-temporal scale modelling and solution present considerable challenges [19]. Resource planning problems involve multi-year time horizons, requiring consideration of investment recovery and long-term trends, while operational issues involve daily/hourly scheduling optimization. Existing studies often address these two types of problems separately, making it difficult to ensure the economic effectiveness of planning schemes in actual operation. This study proposes establishing the intrinsic relationship between long- and short-term time scales through a bi-level model. However, such bi-level optimization problems exhibit non-convex and nonlinear characteristics, resulting in high computational complexity. Algorithm design must therefore carefully balance accuracy and efficiency.

Furthermore, from the perspective of equipment operation and maintenance, overly frequent power switching or repeated large-magnitude adjustments may accelerate the wear and tear of electrical and mechanical components, compromising production continuity and equipment service life. Therefore, when constructing an optimization model for industrial loads participating in grid regulation, it is essential to strike a balance between meeting system flexibility requirements and ensuring the safe and stable operation of equipment through well-designed regulation strategies.

In summary, the research must balance physical realism with computational tractability in modelling, and combine heuristic algorithms with mathematical optimization strategies in solution approaches, thereby providing economical and feasible deployment solutions for flexible resources in power grids. Thus, to address the flexible resource planning problem under the coordinated regulation of industrial loads and energy storage systems in urban power grids, this paper proposes constructing a bi-level optimization model based on long- and short-term time scale coupling. This model comprehensively considers the physical coupling and economic objectives across investment and operational stages, systematically addressing issues of resource siting, capacity allocation, and regulation capability assessment.

In terms of the model structure, the outer-level model aims to minimize the total system cost over the resource planning period. Its primary decision variables include the siting and adjustable capacity of industrial flexible loads, as well as the installation sizing and siting of energy storage systems. A key constraint is that grid stability must be maintained even under N-1 contingency conditions. Simultaneously, the outer-level model incorporates flexible resource investment costs, depreciation costs, and projected operational economic metrics. The decisions from the outer-level model will be transmitted as input parameters to the inner-level model.

Due to the cumulative nature of energy storage capacity, it is essential to build upon the solution from the outer-level model to obtain accurate resource siting and capacity configuration [20-21]. The inner-level operational model simulates the actual system operation process under different load and storage schemes against the background of typical operational day scenarios. Its specific objective is to minimize the overall planning cost, encompassing the investment costs of flexible resources, balancing costs induced by renewable energy output fluctuations, and operational strategies for energy storage charging/discharging and load response. The accuracy of the operational simulation is enhanced by setting representative typical day scenarios (such as peak load days, low-wind days, high-solar days, etc.).

The outer and inner levels are solved interactively through an iterative process. The outer level provides a preliminary resource allocation scheme, while the inner level returns the detailed optimal operational costs of this scheme across various operational scenarios. This process iterates continuously until converging to an overall optimal resource deployment plan for the system. Meanwhile, to enhance solution efficiency, a hybrid heuristic approach (such as genetic algorithms and particle swarm optimization) combined with convex optimization methods is planned to decompose and perform global search on nonlinear, non-convex problems.

The advantage of this scheme lies in closely integrating the layout of flexible resources during the planning period with the actual response capabilities during the operation period, enabling a true reflection of the economic and feasibility of different schemes, and providing theoretical support and engineering guidance for constructing a flexible operation system of "source-load-storage" collaborative interaction in urban power grids.

2. A Bi-level Optimization Model for Multi-Timescale Flexibility Requirements in Urban Power Systems

To ensure the secure and economic operation of urban power grids under high-penetration renewable energy integration, establishing a scientifically sound optimization model for flexible resource planning becomes crucial. This paper addresses the synergistic planning of flexible resources in urban power grids, focusing on energy storage systems and industrially adjustable loads, with particular emphasis on how resource allocation impacts operational economics. Guided by the principle of life-cycle cost optimization, the proposed model adopts a bi-level optimization structure that separately characterizes cost components in long-term resource allocation phases and short-term resource allocation phases. All costs are uniformly converted into levelized cost per kWh (¥/kWh) to facilitate subsequent model normalization and cost-benefit comparison.

The model consists of two distinct levels. The outer-level model prioritizes securing power flow stability under multiple contingency scenarios, determining the minimum required regulation capacity at each candidate node—representing the "essential regulatory resources." The inner-level model then builds upon this foundational capacity to formulate dispatch strategies for typical operational days. By optimizing resource utilization pathways and implementing necessary resource supplementation, it minimizes configuration costs and renewable energy curtailment expenses, thereby maximizing resource utilization efficiency.

Given their divergent objectives, variable boundaries, and temporal scales, the two levels require hierarchical modeling to enhance solution reliability and practical applicability.

2.1. Outer-Level Model: Emergency-Driven Minimal Resource Configuration

The outer-level model focuses on the secure operational requirements of urban power grids under typical N-1 contingency scenarios (such as line tripping and equipment failures). By analysing power flow distributions under multiple potential contingency conditions, it determines the minimum required capacity of energy storage and adjustable loads at each node to prevent post-contingency line power flow violations. The objective function is formulated as follows:

$$\min \sum_i (\alpha_i C_{sto,i} + \beta_i C^{up}_{load,i} + \gamma_i C^{down}_{load,i}) \quad (1)$$

Among them, α_i, β_i, and γ_i denote the unit capacity configuration costs; $C_{\text{sto},i}$, $C^{\text{up}}_{\text{load},i}$, and $C^{\text{down}}_{\text{load},i}$ represent the energy storage and adjustable load capacities (including up-regulation and down-regulation) to be configured at node i.

This model conducts power flow analysis under all preset fault scenarios. Supported by the voltage instability configuration capability, it ensures no line power limit violation or maximum power injection issue at nodes occurs. It outputs the minimum resource configuration inner limit for each node, providing a "safety boundary" for the inner-layer model.

2.2. Inner-Level Model: Economics-Driven Resource Dispatch and Supplemental Decision-Making

The inner-level model builds upon the minimum resource allocation provided by the outer-level model and further incorporates forecasts of typical daily load and renewable energy output to develop a time-period-based dispatch strategy for flexible resources. While ensuring the satisfaction of flexible demand, it simultaneously considers the losses associated with wind and solar curtailment. By evaluating the trade-offs of implementing supplemental resource allocation, the model achieves optimal configuration efficiency. The objective function is formulated as follows:

$$\min \sum_i (\alpha_i C'_{sto,i} + \beta_i C'^{up}_{load,i} + \gamma_i C'^{down}_{load,i}) + \sum_t \varphi_t P^t_{aba} \quad (2)$$

Among them, $C'_{\text{sto,i}}$, $C'_{\text{upload,i}}$, $C'_{\text{download,i}}$ refer to the energy storage and adjustable load capacity that need to be configured to meet the flexibility demands of the urban power grid; φ_t represents the unit penalty cost for curtailment, reflecting the utilization value of renewable energy; P_t^{aba} is the amount of wind and solar power curtailment.

Compared to the outer-layer model, the configuration of the inner-layer model is relatively flexible. Since it can utilize *wind and solar curtailment* to balance flexibility demands, the allocation of flexibility resources is more susceptible to policy and subjective decision-making. In contrast, the outer-layer model is premised on the stable operation of the power grid. The flexibility resources planned in this layer aim to ensure frequency, voltage, and other stability aspects under grid contingencies, making its configuration more rigid.

This model dynamically dispatches the configured resources to meet time-varying flexibility regulation demands and determines whether additional regulatory resources are needed based on the cost of curtailment. The final outputs include the regulation paths for energy storage/load at each time period, as well as decisions on whether additional resource allocation is required, how much is needed, and at which nodes it should be added.

3. Constraint Analysis and Structural Comparison of the Bi-level Planning Model for Urban Power Grids with Adjustable Nodes

In the bi-level model proposed in this paper, the outer-level model focuses on the security of resource allocation under fault emergency conditions, while the inner-level model is dedicated to optimizing dispatch strategies and economic efficiency during typical operational days based on the allocated resources. Although both models revolve around energy storage and adjustable industrial loads, significant differences in their objective orientation, optimization variables, time scales, and input data result in constraint structures that share commonalities while also exhibiting critical distinctions. This chapter will systematically analyse the structural characteristics of the bi-level model from the perspective of constraints, thereby further clarifying why they cannot be merged.

3.1. Constraints of the Outer-Level Model

The core objective of the outer-level model is to minimize the overall configuration cost of energy storage and adjustable loads under multiple typical fault scenarios (e.g., N-1 line tripping contingencies), while ensuring post-fault power flow security of the system.

To ensure that the model's optimization results possess both physical feasibility and engineering implementability,

the constraints imposed by actual engineering conditions on their power regulation capabilities must be fully considered when deploying energy storage systems and industrially adjustable loads in urban power grids. Consequently, in constructing the bi-level model, it is necessary to introduce operational boundary constraints derived from node assessment results and equipment specifications. These constraints encompass multi-dimensional metrics such as the power regulation capacity per node and per time interval, power flow security, and power balance.

For each node and time interval, the regulation amount of industrial load must not exceed the quantified adjustable capacity obtained through assessment; that is, load regulation is constrained by the upward (positive limit) and downward (negative limit) regulation capabilities after retrofitting. The charging/discharging of energy storage equipment at each node is similarly limited by power transfer constraints, and the maximum power of storage at different nodes can be set according to the capacity of the connection point, line access capability, or equipment specifications. These constraints ensure the practical implementability of power operations. Based on preliminary surveys and equipment retrofitting assessments, they provide the model with realistic, physically reasonable regulation boundaries.

$$-P_{\text{load},i}^{\text{down}} \le P_{\text{load},i}^{\text{adj},t} \le P_{\text{load},i}^{\text{up}}, \forall i \in \{1,2,\ldots,n\}, \forall t \in \{1,2,\ldots,T\} \quad (3)$$

$$-P_{\text{sto},i}^{\text{cap}} \le P_{\text{sto},i}^{t} \le P_{\text{sto},i}^{\text{cap}}, \forall i \in \{1,2,\ldots,n\}, \forall t \in \{1,2,\ldots,T\} \quad (4)$$

Among them, $P_{\text{load},i}^{\text{down}}$, $P_{\text{load},i}^{\text{up}}$, and $P_{\text{sto},j}^{\text{cap}}$ represent the upper and lower power limits, respectively.

In the outer-layer model, to ensure that the urban power grid maintains safe operation capability under typical fault scenarios (such as line N-1 tripping, equipment failure), power flow analysis must be performed for each fault scenario $s \in S$, mandating that the power of all lines does not exceed their rated capacity:

$$| P_{ij}^{s} | \le P_{ij}^{max}, \forall (i,j) \quad (5)$$

Among them, P_{ij}^{s} denotes the line power under different fault scenarios s, and $P_{ij}^{\max}$ refers to the line capacity.

For the operational reliability of the urban power grid, it is necessary to ensure the power balance of the entire network in each time period — i.e., the charging/discharging volume of energy storage devices, industrial load regulation volume, and the flexibility demand of the network should match each other. This ensures the real-time energy supply-demand balance of all nodes in each time period, avoiding system "shortage" or regulation "excess":

$$\sum_{j} P_{ij}^{s} + \Delta P_{i}^{s} = P_{load,i} + P_{sto,i}, \forall i, s \quad (6)$$

Among them, ΔP_i^s represents the power deficit under different fault scenarios s, while $P_{\text{load},j}$ and $P_{\text{sto},i}$ denote the load regulation power and energy storage charging/discharging power, respectively.

Through power flow analysis and emergency dispatch simulation for multiple typical fault scenarios, the outer-layer model determines the minimum configuration capacities of energy storage and industrial load resources at each node — this ensures the power flow security and operational stability of the urban power grid under extreme operating conditions. The configuration results in this part reflect the "safety boundary" of system operation; they are passed to the inner-layer model as parameter inputs, serving to constrain the lower limit of resource allocation.

3.2. Constraints of the Inner-Level Model

The inner-layer model further conducts optimization decisions centered on the temporal flexibility requirements of typical operation days. On the one hand, it evaluates whether supplementary resource allocation is necessary to enhance flexibility redundancy; on the other hand, it formulates optimal dispatch paths, makes full use of existing resources to address renewable energy fluctuations and load uncertainty, minimizes operational losses such as wind-solar curtailment as much as possible, and improves the overall operational economy and flexibility.

In this model, although the actual adjustable capacity of industrial flexible loads is based on prior retrofitting assessments, their "resource boundaries" in the optimization are no longer directly determined by their flexibility potential. Instead, they are constrained by the minimum configuration results derived from the contingency analysis in the outer-level model. This approach ensures that, in any dispatch scheme, the regulation resources always meet the minimum requirements for secure system operation, providing stronger engineering feasibility and safety assurance.

$$\begin{aligned} C'^{down}_{load,t} &\le P^{t}_{load,i} \le C'^{up}_{load,t} \\ C^{down}_{load,t} &\le C'^{down}_{load,t} \le C^{downMax}_{load,t} \\ C^{up}_{load,t} &\le C'^{up}_{load,t} \le C^{upMax}_{load,t} \end{aligned} \quad (7)$$

Among them, $C_{\text{load},j}^{\text{down}}$ and $C_{\text{load},t}^{\text{up}}$ are the flexibility resource retrofitting volumes to be determined in the inner-layer model, while $P_{\text{load},i}^{t}$ refers to the load regulation power under typical daily operation.

From the perspective of modeling energy storage resources, the configuration of energy storage must not only meet the minimum capacity threshold determined by the outer-level model to ensure emergency response capability in contingency scenarios, but also incorporate its dynamic operational constraints in the inner-level dispatch to guarantee the rationality and sustainability of the operation process. Specifically, during the dispatch of a typical day, the state of energy storage is subject to constraints of the state of charge (SOC): on the one hand, the SOC must not exceed the maximum available capacity or fall below the minimum allowable value at any time, preventing overcharge or over-discharge; on the other hand, to ensure continuity in rolling optimization or multi-day operation, the energy storage system must satisfy a periodic constraint that the SOC at the beginning and end remains consistent, namely:

$$E_i^{t+1} = E_i^t + P_{sto,i}^t \cdot \Delta t$$
$$E_i^0 = E_i^T \tag{8}$$
$$0 \le E_i^t \le C'_{sto,i}, C_{sto,i} \le C'_{sto,i}$$

Among them, E_i^t denotes the energy storage inventory value of node i at time t, and $C'_{\mathrm{sto},i}$ is the energy storage configuration to be determined in the inner-layer model. This constraint ensures that the energy storage still retains sufficient energy at the end of each typical day, avoiding the depletion of energy storage resources due to short-term dispatch strategies (which would affect subsequent regulation capability). It reflects the reasonable characterization of the dynamic regulation characteristics of energy storage devices throughout their lifetime.

Unlike the outer-level model, which primarily focuses on rigid power balance and flow security under fault scenarios, the inner-level model incorporates renewable energy fluctuation scenarios and controllability differences, no longer mandating full absorption of wind and solar power generation. To this end, the model introduces adjustable wind and solar curtailment variables into the nodal power balance constraints, allowing the system to moderately curtail a portion of renewable energy output when resources are insufficient or regulation costs are prohibitively high, thereby reducing overall operational stress and unnecessary adjustment costs. Specifically, the nodal power balance constraint in the inner-level model is reformulated as:

$$\sum_j P_{ij}^t + \Delta P_i^t = P_{load,i}^t + P_{sto,i}^t + P_{aba,i}^t, \forall i,t \tag{9}$$

Among them, ΔP_i^t denotes the power deficit caused by differences in generator output, wind-solar power generation, and load power across different time periods and nodes; $P_{\mathrm{aba},i}^t$ refers to the wind-solar curtailment volume of node i in time period t. This processing method not only enhances the flexibility and practical adaptability of the model, but also embodies the "flexible tolerance mechanism" of the urban power grid for renewable energy fluctuations — making resource allocation and dispatch more economically efficient and engineering-rational. This setting is one of the distinctive features that distinguishes the inner-layer model from the outer-layer model.

Meanwhile, in typical operational day scenarios, the urban power grid must still dynamically respond to fluctuations in wind and solar output as well as load uncertainty at each time interval. Therefore, it must satisfy the balance constraint for flexibility requirements. This constraint ensures that, throughout the time-series operation, the system can meet the forecasted flexibility adjustment demands through energy storage charging/discharging, industrial load regulation, and, when necessary, wind and solar curtailment, thereby avoiding energy shortfalls or excessive regulation capacity redundancy.

$$\sum_i (P_{sto,i}^t + P_{load,i}^t) \ge P_{flex}^{up,t}, \forall t$$
$$\sum_i (-P_{sto,i}^t - P_{load,i}^t) \ge P_{flex}^{down,t}, \forall t \tag{10}$$

Among them, P_{fle}^t refers to the flexibility resource demand. This constraint is one of the cores of the inner-layer model: it ensures that the configuration and dispatch of regulation resources have coverage and adaptability to typical daily operations, while also providing a basis for the trade-off between regulation costs and curtailment costs in the objective function. By introducing this constraint, the model can simulate how flexibility resources respond to renewable energy output fluctuations in actual operation, thereby improving the operational reliability and economic efficiency of the urban power grid.

4. Case Study

As shown in Figure 1, this paper adopts a six-node system for simulation and validation. The system features G1 (Node 1) and G2 (Node 2) as main power injection points, both capable of drawing electricity from external sources to form a multi-source support structure. They are connected to other nodes within the system via transmission lines, providing the foundation for regional power supply. By leveraging the mutual power supply potential of the dual power sources , the system enhances power supply stability and reliability, enabling them to complement each other and ensure continuous electricity supply in the event of a single source failure or output fluctuation.

The lines between nodes form a meshed topology, creating multiple sub-networks. Relying on this ring configuration, the system enables load transfer and flexible power flow control. When a line fault occurs or a power source output changes, the ring network allows switching of power paths to maintain continuous electricity transmission, thereby improving system redundancy and fault tolerance.

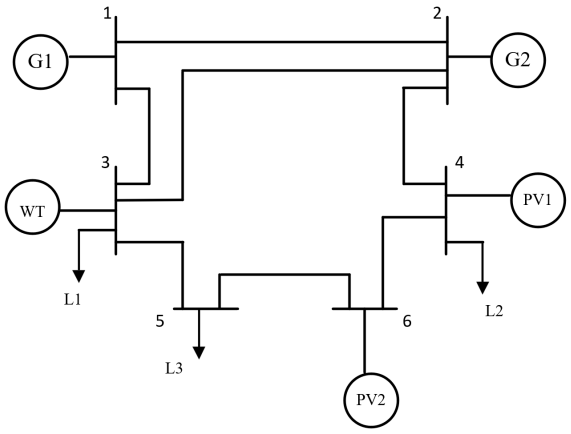

Figure 1. Topology Diagram of the Six-Node System

Nodes 3 and 4 serve as critical hubs within the system. Node 3 is connected to G1, WT, L1, and other nodes, aggregating power from both wind and thermal generation, and distributing it to L1 and downstream nodes. Node 4 is

linked to G2, PV1, L2, and subsequent nodes, integrating power from thermal and photovoltaic sources and delivering it outward. Leveraging their connections to multiple power sources and loads, both nodes undertake the tasks of power flow regulation and multi-directional interconnection. They balance output differences among diverse generation sources, coordinate to meet regional load demands, and ensure the orderly flow of power throughout the system.

Table 1. Typical Daily Load Power (MW) Data for the Node System

Node No	Industrial Type	Installed Capacity (MVA)
3	steel	4.5
3	cement	4.0
4	glass	1.5
4	textile	2.0
5	electronics factory	1.8
5	steel	4.8

The intermittency of new energy nodes necessitates that the system cope with power fluctuations. The ring-network topology and conventional power sources (G1, G2) provide the foundation for flexibility regulation. On the generation side, G1 and G2 can adjust their output to accommodate changes in new energy generation. On the network side, the ring-network structure enables redistribution of power flow, transferring the impact of power fluctuations. On the load side, although demand is passive, load transfer via the ring-network can also adapt to certain load variations. However, due to the fluctuating nature of new energy, relying solely on conventional power sources and the ring-network may not fully stabilize power disturbances. Therefore, it is essential to combine energy storage configurations—such as deploying storage at nodes with high new energy concentration or critical load nodes. Energy storage can charge to absorb surplus energy and discharge to compensate for power deficits, thereby further unlocking the system's regulation potential, enhancing flexibility, and ensuring stable power supply.

The industrial load access status at different nodes and typical daily power data for specific nodes are shown in Tables 1 and 2, respectively.

Table 2. Industrial Load Access Conditions at Different Nodes

Time	Node 3: Steel Load	Node 3: Cement Load	Node 4: Glass Load	Node 4: Textile Load	Node 5: Electronics Factory Load	Node 5: Steel Load
0:00	3.8	3	1.3	2.4	1.5	3.9
1:00	3	3.2	1.5	2	1.5	4.3
2:00	4	3.3	1.4	2	1.4	4.1
3:00	3.8	2.8	1.5	1.9	1.7	4.3
4:00	3.5	3.2	1.5	2	1	4.7
5:00	3.8	2.8	1.4	2	1.2	3.6
6:00	3.5	2.8	1.5	2	1.6	3.4
7:00	3.7	3.1	1.5	3.2	1	4.2
8:00	3.9	3.1	1.4	2	1.5	4.3
9:00	3.4	3.9	1.3	2	1.7	4.1
10:00	3.1	3.0	1.3	2	1.6	3.7
11:00	3.2	3.1	1.4	2	1.4	4
12:00	3.2	3.2	1.3	2	1.7	4.3
13:00	3.8	3.0	1.4	2.0	1.3	3.8
14:00	3.0	3.1	1.3	1.9	1.6	4.2
15:00	3.4	3.0	1.3	2.0	1.6	3.7
16:00	3.8	3.2	1.4	2	1.4	4.4
17:00	3.9	3.1	1.3	2	1.6	4.1
18:00	3.5	3.3	1.3	2	1.2	4.3
19:00	3.0	3.2	1.3	1.1	1.6	3.8
20:00	2.8	3.2	1.3	2.8	1.5	4.0
21:00	3.1	3.2	1.4	2.2	1.6	3.9
22:00	3.7	3.2	1.4	1.5	1.5	4.4
23:00	4.2	3.3	1.4	2.3	1.4	4.5

From the load data of the 6-node system, it is evident that the load characteristics of each node differ significantly and are highly correlated with industrial types. Node 3 is dominated by heavy industrial loads such as steel and cement. The daily fluctuation of the steel load is 1.2 MW (from 3.0 to 4.2 MW), and the cement load fluctuates by 0.5 MW (from

2.8 to 3.3 MW). After superposition, the overall load base is large, maintaining a high level during daytime production hours (7:00-20:00), with only localized peak-valley staggering (e.g., steel peaks at 4.2 MW at 23:00 while cement is at 3.3 MW). This profile makes it suitable for providing stable regulation support. The load at Node 4 is primarily from glass and textile industries. The glass load is exceptionally stable (1.3-1.5 MW), while the textile load shows more noticeable fluctuations (1.1-3.2 MW), peaking at 7:00 and reaching a valley at 19:00. This allows leveraging the flexibility of the textile load to respond to short-term fluctuations. Node 5 features a mixed load of an electronics factory and steel production. The electronics factory load is light and flexible (1.0-1.7 MW), whereas the steel load is heavy and exhibits large fluctuations (3.4-4.7 MW). When steel peaks at 4.7 MW at 4:00, it can be balanced by coordinating with an increase in the electronics factory load, forming a "light-heavy complementary" regulation potential.

The periods from 7:00 to 9:00 and 17:00 to 20:00 are load peaks. Concentrated high loads occur at Node 3 (cement, 3.9 MW), Node 4 (textile, 3.2 MW), and Node 5 (steel, 4.2 MW). Combined with residential electricity consumption and new energy output fluctuations, this necessitates the dispatch of industrial loads for peak shaving (e.g., reducing the textile load at 7:00 and moderately adjusting down the steel load). The periods from 0:00 to 6:00 and around 19:00 are load valleys. Loads such as textile at Node 4 (1.1 MW) and steel at Node 3 (3.0 MW) operate at low levels, allowing for strategies like guiding heavy industry to preheat or store energy and light industry to start backup production lines for valley filling, thereby reducing new energy curtailment. These characteristics provide data support for the bi-level grid planning model: the outer-level contingency analysis can rely on the stable regulation from heavy industry at Nodes 3 and 5 to ensure power flow security, while the inner-level economic dispatch can utilize the rapid response capabilities of the textile industry at Node 4 and the electronics factory at Node 5 to optimize costs.

The flexibility requirement data for the 6-node system, resulting from unstable new energy output, are presented in Table 3 below:

This is the body text with indent. This is the body text with indent. This is the body text with indent. This is the body text with indent. This is the body text with indent. This is the body text with indent. This is the body text with indent. This is the body text with indent. This is the body text with indent. This is the body text with indent. This is the body text with indent. This is the body text with indent.

Table 3. Typical Daily Flexibility Requirements (MW) Data of the Node System

Time	Node 3		Node 4		Node 6	
	Downward Regulation	Upward Regulation	Downward Regulation	Upward Regulation	Downward Regulation	Upward Regulation
0:00	6.01	5.88	6.63	6.5	3.23	4.16
1:00	5.66	5.72	6.11	6.6	3.19	3.86
2:00	5.58	5.72	6.43	6.66	3.01	3.98
3:00	5.73	5.34	6.42	5.62	2.95	4.21
4:00	5.58	5.82	6.38	6.67	2.93	4.02
5:00	5.34	5.66	6.26	6.71	3.27	3.95
6:00	5.63	5.88	6.75	6.81	3.42	4.2
7:00	5.84	6.04	6.22	6.37	3.02	3.96
8:00	5.98	6.04	6.93	6.33	3.2	4.25
9:00	5.75	5.61	6.66	6.18	2.98	4.51
10:00	5.71	6.12	6.49	6.31	3.09	3.8
11:00	5.47	5.81	6.76	6.84	3.39	4.25
12:00	5.88	5.58	6.15	6.8	3.04	4.21
13:00	5.87	5.46	6.23	7.04	3.4	3.8
14:00	5.46	5.62	6.68	6.77	3.06	4.03
15:00	5.71	5.73	7.12	7.14	3.23	3.93
16:00	5.51	6.24	6.28	6.64	3.3	4.01
17:00	5.8	5.59	6.86	6.58	3.02	4.19
18:00	5.96	5.35	6.25	6.04	2.97	4.29
19:00	6.31	5.65	6.93	7.08	3.2	4.19
20:00	5.68	5.45	6.49	6.34	2.81	4.22
21:00	6.18	5.28	6.71	6.62	3.24	4.28
22:00	6.05	5.62	6.89	6.78	2.84	3.9
23:00	5.78	5.53	6.35	6.66	3.35	4.31

This data reflects the flexibility requirements triggered by fluctuations in new energy output. Downward regulation corresponds to the need to reduce the output of flexible resources to maintain balance when new energy suddenly

decreases, while upward regulation addresses the need to absorb or transfer redundant power when new energy is in surplus.

From the perspective of node differences, the distribution of requirements is strongly correlated with new energy integration and industrial load characteristics. Node 4 has the highest demand for both downward and upward regulation, with a downward regulation peak of 7.12 MW (at 15:00) and an upward regulation peak of 7.14 MW (at 15:00). This node has a high proportion of new energy integration combined with the electricity consumption patterns of its glass and textile loads, necessitating greater regulation capacity to counteract new energy fluctuations. Node 3 has the next highest demand, with a downward regulation peak of 6.31 MW (at 19:00) and an upward regulation peak of 6.24 MW (at 16:00). This matches the continuous power demand of its heavy industrial steel and cement loads, requiring precise reduction of flexible resource output when new energy decreases to avoid impacting production. Node 6 has the lowest demand, with a minimum downward regulation of 2.81 MW (at 20:00) and a maximum upward regulation of 4.51 MW (at 9:00), likely because this node has less new energy integration and higher load stability, resulting in weaker dependence on regulation.

In terms of temporal patterns, the variation in requirements closely aligns with the characteristics of new energy output. During the daytime (7:00-17:00), significant fluctuations in photovoltaic output cause frequent rises and falls in demand at Nodes 4 and 3. For example, at 15:00, Node 4 experiences bidirectional regulation demands both exceeding 7 MW due to sudden increases or decreases in photovoltaic output. From evening to night (18:00-23:00), wind power fluctuations may occur. At 19:00, the downward regulation demand at Node 3 reaches 6.31 MW, corresponding to a sudden drop in new energy, requiring a rapid reduction in flexible resource output to balance supply and demand. During the early morning hours (0:00-6:00), new energy output is stable, and the demand at each node is relatively gentle. For instance, at 3:00, Node 3 has a downward regulation demand of 5.73 MW and an upward regulation demand of 5.34 MW, indicating lower regulation pressure.

This data provides crucial support for the bi-level planning model. The outer-level model can set stricter contingency security constraints (such as line power limits during sudden new energy decreases) for high-demand scenarios at Nodes 3 and 4, ensuring power flow security when flexible resources are reduced or supplemented. The inner-level model can optimize strategies based on time-varying demands. For example, during daytime periods of new energy fluctuation, it can call upon the textile load at Node 4 for rapid response regulation. During nighttime periods of stable new energy output, it can guide the heavy industrial load at Node 3 to participate in flexible resource dispatch, achieving a balance between new energy accommodation and grid economic efficiency.

The inherent load retrofit capability data for the corresponding 6-node system are presented in Table 4.

Table 4. 6 Typical Daily Flexibility Requirements (MW) Data of the Node System

	Node 3		Node 4		Node 5	
Time	Peak Shaving Capability (MW)	Valley Filling Capability (MW)	Peak Shaving Capability (MW)	Valley Filling Capability (MW)	Peak Shaving Capability (MW)	Valley Filling Capability (MW)
0:00	1.23	0.18	0.2128	0.0135	1.0331	0.0968
1:00	0.23	0.2	0.11	0.02	0.348	0.1695
2:00	0.47	0.22	0.08	0.02	0.3798	0.0972
3:00	0.61	0.16	0.13	0.02	0.3682	0.1229
4:00	0.86	0.11	0.09	0.0232	0.4006	0.0979
5:00	0.48	0.15	0.07	0.208	0.41	0.2031
6:00	0.95	0.16	0.06	0.232	0.499	0.1686
7:00	0.74	0.15	0.114	0.0131	0.3839	0.1934
8:00	1.44	0.15	0.16	0.0196	0.499	0.1315
9:00	0.98	0.22	0.1216	0.0227	0.507	0.1923
10:00	1.01	0.13	0.1368	0.0227	1.0383	0.0888
11:00	0.73	0.13	0.114	0.025	0.2466	0.2278
12:00	0.57	0.16	0.0608	0.0185	0.836	0.0833
13:00	0.87	0.15	0.114	0.025	0.5985	0.1842
14:00	1.08	0.13	0.1976	0.0194	0.5231	0.2001
15:00	0.93	0.14	0.2052	0.0228	0.898	0.1501
16:00	0.79	0.18	0.1748	0.0195	0.4725	0.1377
17:00	0.99	0.18	0.0684	0.0249	0.5649	0.2237
18:00	0.76	0.16	0.1520	0.0216	0.6512	0.1939
19:00	0.99	0.17	0.1292	0.0214	0.7913	0.1232
20:00	0.81	0.15	0.1824	0.0098	0.6454	0.1590

Time	Node 3		Node 4		Node 5	
	Peak Shaving Capability (MW)	Valley Filling Capability (MW)	Peak Shaving Capability (MW)	Valley Filling Capability (MW)	Peak Shaving Capability (MW)	Valley Filling Capability (MW)
21:00	0.72	0.16	0.0760	0.0114	1.0320	0.1890
22:00	0.83	0.17	0.0760	0.0264	0.5365	0.1341
23:00	0.27	0.22	0.1292	0.0120	0.3179	0.2090

This data reflects the peak shaving (reducing power during new energy surplus or load peaks) and valley filling (increasing power during new energy shortage or load valleys) retrofit potential of industrial loads at Nodes 3, 4, and 5. It is directly linked to the reserve of regulation resources available to the grid for responding to new energy fluctuations.

Node 3 exhibits the strongest peak shaving capability, with a peak of 1.44 MW and a sustained range of 0.7–1.0 MW during most periods, while its valley filling capability is relatively weak (0.11–0.22 MW). This aligns with its heavy industrial characteristics dominated by steel and cement. Due to the large base load of heavy industry, considerable peak shaving potential can be unlocked through production process optimizations (e.g., adjusting rolling schedules, pausing non-critical equipment). However, valley filling requires additional energy consumption (e.g., equipment preheating), leaving limited room for retrofit. Node 5 shows the next strongest peak shaving capability, with a peak of 1.0383 MW and valley filling ranging from 0.0888 to 0.2278 MW. Leveraging the flexible adjustment of the electronics factory combined with minor retrofits to the steel load, it forms a "light-heavy synergy" advantage in peak shaving. Node 4 has the weakest regulation capability, with peak shaving only between 0.06 and 0.2052 MW and valley filling between 0.0098 and 0.232 MW. This is due to the continuous production nature of glassmaking and limited retrofit potential of the textile load, allowing it to provide only auxiliary regulation.

Temporally, peak shaving capability closely aligns with load peak periods and times of new energy fluctuation. During intervals such as 8:00 (Node 3: 1.44 MW), 10:00 (Node 5: 1.0383 MW), and 14:00 (Node 3: 1.08 MW)—which correspond to previously identified flexibility requirement peaks (e.g., Node 4 downward regulation of 6.93 MW at 8:00)—industrial loads can provide peak shaving to absorb surplus new energy power. At 21:00, Node 5's peak shaving capability of 1.032 MW matches the flexibility demand during 19:00–21:00 (Node 3 downward regulation of 6.31 MW), thereby alleviating grid peak regulation pressure. Valley filling capability remains relatively stable throughout the day, with only slightly higher values around 5:00–6:00 (Node 4: 0.208–0.232 MW) and 11:00 (Node 5: 0.2278 MW), which can assist energy storage in valley filling during early morning hours of stable new energy output (e.g., 3:00–6:00) and help reduce curtailment.

In terms of alignment with flexibility requirements, the peak shaving capabilities of Nodes 3 and 5 can effectively cover partial demand gaps. For instance, at 8:00, Node 3's peak shaving capability of 1.44 MW can address about 21% of Node 4's downward regulation demand (6.93 MW); at 21:00, Node 5's peak shaving capability of 1.032 MW can cover approximately 16% of Node 3's downward regulation demand (6.18 MW). However, overall, the valley filling capabilities across nodes are generally lower than the upward regulation demands (e.g., Node 4's upward regulation demand of 7.04 MW at 13:00 versus its valley filling capability of only 0.025 MW), necessitating reliance on energy storage or conventional power sources for supplementation. This data provides a practical basis for the bi-level planning model: the outer-level model can treat the peak shaving capabilities of Nodes 3 and 5 as core "safety margin" reserves to ensure regulation redundancy during contingencies with sudden new energy drops; the inner-level model can prioritize dispatching the peak shaving resources of Nodes 3 and 5 to meet typical daily demands, utilize Node 4 for auxiliary regulation, and simultaneously target enhancements in valley filling retrofits (e.g., increasing capacity of textile load during valleys at Node 4) to optimize the economic efficiency of resource allocation.

For the flexibility resource allocation planning under different scenarios, based on the bi-level planning model for multi-timescale flexibility requirements in urban power systems proposed in this paper, the calculated results are presented in Table 5.

Table 5. Flexible Resource Allocation Planning in Different Scenarios

Scenario	Flexibility Resource Allocation Plan	Node 1	Node 2	Node 3	Node 4	Node 5	Node 6
Real-Time Control	Energy Storage Configuration / MWh	9.6	0	0	16.3	1.8	9.5
	Load Down-Regulation Capacity Retrofit / MW	0	0	0.8	0.2	0.7	0
Peak Shaving	Energy Storage Configuration / MWh	5.6	0	0	9.11	0	0

	Load Down-Regulation Capacity Retrofit / MW	0	0	1.1	0.2	0	0
Valley Filling	Energy Storage Configuration / MWh	6.2	0	0	10	0	0.1
	Load Up-Regulation Capacity Retrofit / MW	0	0	0.18	0.23	0.22	0

This case study focuses on three core scenarios—real-time control, peak shaving, and valley filling—and specifies the nodal distribution of energy storage configuration (MWh) and load retrofit (MW).

Real-time control scenario: This scenario requires rapid response to sudden increases or decreases in new energy output (e.g., abrupt changes in photovoltaic output or wind gusts). The configuration prioritizes "energy storage as the main resource, supplemented by load reduction," emphasizing flexibility and timeliness. Node 4 (16.3 MWh) is the core, far exceeding other nodes. Consistent with earlier data, Node 4 has the highest flexibility requirement (downward regulation peak 7.12 MW, upward regulation peak 7.14 MW), but its load retrofit capability is extremely weak (peak shaving only 0.06–0.2052 MW). Thus, large-capacity energy storage is needed to handle real-time regulation tasks. Nodes 1 (9.6 MWh) and 6 (9.5 MWh), as power-source/interconnection nodes, deploy energy storage to balance regional power fluctuations (e.g., Node 1 is connected to G1 and must buffer interaction impacts between external power sources and internal loads). Node 5 (1.8 MWh) has a relatively small energy storage size because its load retrofit capability is strong (peak shaving up to 1.0383 MW); here storage only plays an auxiliary role. Load reduction retrofits are concentrated at Node 3 (0.8 MW), Node 4 (0.2 MW), and Node 5 (0.7 MW). Node 5 has previously demonstrated strong peak-shaving potential, and its retrofit amount matches its available retrofit space. Although Node 4 has a small retrofit amount (0.2 MW), it can form a "fast-response combination" with its 16.3 MWh energy storage: when new energy drops abruptly, slight load adjustment buys time first, followed by deeper regulation from storage, ensuring real-time power balance.

Peak-shaving scenario: This scenario aims to address load peaks (e.g., 7:00-9:00, 17:00-21:00) and new-energy surplus (e.g., midday full photovoltaic output). The configuration focuses on "energy storage at high-demand nodes + load reduction at core nodes." Only Nodes 1 (5.6 MWh) and 4 (9.11 MWh) are configured with energy storage. Node 4 is the core of peak-shaving demand (downward regulation 6.93 MW at 8:00); its 9.11 MWh storage can absorb redundant power during peak periods. Node 1, connected to G1, uses storage to smooth interaction fluctuations between conventional power sources and industrial loads (e.g., mismatches between G1 output adjustment and the high load at Node 3). Nodes 3 and 5 are not equipped with storage because their existing load retrofit capabilities can already cover part of the peak-shaving demand (Node 3 peak shaving up to 1.44 MW), avoiding redundant investment. Load reduction retrofits are applied at Node 3 (1.1 MW) and Node 4 (0.2 MW). The retrofit amount at Node 3 is higher than in the real-time control scenario (0.8 MW → 1.1 MW) because its heavy-industrial load has a large base during peak-shaving periods (e.g., steel 3.9 MW and cement 3.1 MW at 8:00); a 1.1 MW reduction capability can directly meet about 15 % of Node 3's peak-shaving demand (previously, Node 3's downward regulation peak was 6.31 MW). Node 4's retrofit amount remains the same as in the real-time control scenario because its load retrofit potential is limited and can only provide basic auxiliary support.

Valley-filling scenario: This scenario aims to utilize load valley periods such as early morning hours (0:00–6:00) to absorb surplus new-energy output (e.g., nighttime wind power). The configuration follows the principle of "energy storage as the main resource, supplemented by load increase," addressing the previously identified shortfall in valley-filling capability. Node 4 (10 MWh) remains the core for energy storage, matching its valley-filling demand (e.g., upward regulation of 5.62 MW at 3:00). Nodes 1 (6.2 MWh) and 6 (0.1 MWh) provide supplementary storage. The storage at Node 1 is used to encourage increased generation from G1 during valley periods in coordination with storage charging. Node 6 has minimal storage capacity because its flexibility requirement is low (maximum upward regulation 4.51 MW), requiring only a small amount of storage to balance local fluctuations. Load increase retrofits are applied at Node 3 (0.18 MW), Node 4 (0.23 MW), and Node 5 (0.22 MW). The retrofit amounts are all relatively small, consistent with the earlier conclusion that "valley-filling capabilities are generally weak" (Node 3 peak valley-filling capability 0.22 MW), and load increase retrofits entail additional energy consumption (e.g., preheating of heavy-industrial equipment), necessitating controlled scale. The combined retrofit amount of 0.63 MW can assist energy storage in absorbing new energy during valleys, reducing the cost pressure of storage charging alone (e.g., Node 4's 10 MWh storage coupled with 0.23 MW load increase can alleviate the required charging power).

In summary, Node 4 has the highest energy storage allocation across all scenarios (real-time 16.3 MWh, peak-shaving 9.11 MWh, valley-filling 10 MWh), while its load retrofit amount is consistently the lowest (0.2 MW). The core reason is that this node's load—glass (continuous production) + textile (limited retrofit potential)—has weak retrofit capability, yet its flexibility requirement is the highest. Consequently, large-capacity energy storage is required to compensate for the regulation gap, aligning with the rigid "safety-margin" requirement of the outer-level model for contingency scenarios (e.g., when new energy drops abruptly, storage must rapidly release power to ensure power-flow security). Nodes 3 (steel + cement) and 5 (electronics factory + steel), relying on their stronger load retrofit capabilities, serve as the "main contributors of load

retrofits" in different scenarios: Node 3 provides 1.1 MW retrofit in the peak-shaving scenario (matching its 1.44 MW peak-shaving potential), and Node 5 provides 0.7 MW retrofit in the real-time control scenario (aligning with its 1.0383 MW peak-shaving capability). Energy storage plays only an auxiliary role (e.g., Node 5 real-time control 1.8 MWh), which both reduces storage investment costs (an economic optimization objective of the inner-level model) and enhances coordination efficiency through "fast load response + deep storage regulation." Node 2, as the connection point for G2 (the main power source), inherently possesses conventional generation regulation capability (e.g., G2 can adjust its output). Moreover, earlier data show that this node has no industrial load; its flexibility requirements can be smoothed by generation-side adjustments, eliminating the need for additional energy storage or load retrofits. This reflects the differentiated roles of "source-storage-load" resources.

To further investigate the impact of considering the retrofit potential of industrial load regulation capabilities, this paper conducts scenario simulations based on the six-node system to validate the model's effectiveness.

Scenario 1: Considering only energy storage systems for flexible resource allocation.

In this scenario, the urban power grid does not incorporate any industrially adjustable loads. The system's peak-shaving and regulation tasks are entirely undertaken by energy storage systems. The storage devices charge during valley periods and discharge during peak periods based on electricity prices or load fluctuations, balancing power supply-demand variations and reducing the ramping pressure on thermal power units. This scenario is used to quantify the contribution of energy storage acting alone in flexible regulation to system dispatch optimization, providing a reference for its economic viability and configuration scale.

Scenario 2: Coordinated participation of industrially adjustable loads and energy storage systems in flexible resource allocation.

This scenario represents the most comprehensive configuration for system flexible resources, encompassing both industrially adjustable loads and energy storage systems. The two types of resources act in synergy, each leveraging its strengths across different time scales and operational contexts: load regulation provides rapid response, while energy storage offers energy shifting and system support. Through this scenario, a comprehensive assessment can be made of the improvements in system economy, enhancement of regulation capability, and reduction in operational costs achieved through source-load-storage synergistic optimization, enabling a systematic comparative analysis with the aforementioned scenario.

As shown in Table 6, based on the data from the six-node system, a comparison between energy storage only participation (Scenario 1) and source-load-storage synergy (Scenario 2) clearly reveals the multi-dimensional value brought by industrial load retrofitting. In terms of cost optimization, the total cost of Scenario 1 is 6.18×10^5 yuan, entirely composed of energy storage investment. To meet demands such as real-time control and peak shaving, Node 4 required large-capacity storage configurations (e.g., 16.3 MWh, 9.11 MWh), leading to high costs. In contrast, Scenario 2, by introducing 0.15×10^5 yuan of industrial load retrofitting, reduced energy storage investment to 5.58×10^5 yuan, resulting in a net total cost reduction of 0.45×10^5 yuan (an optimization rate of 7.3%). The peak-shaving retrofitting at Node 3 (steel + cement) and Node 5 (electronics factory + steel) could cover regulation demands originally requiring energy storage (approximately 1.1 MW of retrofitting replaces about 1.5 MWh of storage), achieving the effect of "cost reduction and efficiency enhancement".

Table 6. Flexible Resource Allocation Planning Under Different Scenarios

	Total Cost (CNY)	Energy Storage Investment Cost (CNY)	Load Retrofit Cost (CNY)
Scenario 1	$6.18*10^5$	$6.18*10^5$	0
Scenario 2	$5.73*10^5$	$5.58*10^5$	$0.15*10^5$

It is noteworthy that the operation and maintenance costs of energy storage systems are typically positively correlated with their configured scale and can be represented as a certain proportion of the initial investment cost. In the "storage-load" coordinated scheme (Scenario 2), since activating the regulation potential of industrial loads significantly reduces the required total capacity of energy storage, the corresponding full life-cycle operation and maintenance costs will also decrease proportionally. Therefore, even if Table 6 does not account for the operation and maintenance costs of energy storage, the cost advantage of the "storage-load" coordinated scheme compared to the single energy storage scheme remains valid, and the optimization margin of its total cost (investment + operation and maintenance) may be even more significant.

5. Conclusion

This paper addresses the issue of insufficient operational flexibility in urban power grids under high-penetration new energy integration. Focusing on the synergistic planning of energy storage systems and industrially adjustable loads, it constructs a bi-level optimization model coupled across long- and short-term time scales, aiming to achieve coordinated optimization of security constraints and economic objectives. The outer-level model is centered on ensuring secure grid operation under extreme scenarios such as N-1 contingencies. It determines the minimum required capacity of energy storage and adjustable loads at each node through multi-contingency power flow analysis, thereby establishing a rigid safety boundary for system operation. Building upon this foundation, the inner-level model targets optimal economic performance for typical daily operation. It comprehensively considers fluctuations in new energy output,

load characteristics, and resource regulation costs to dynamically optimize energy storage charging/discharging strategies, industrial load regulation pathways, and necessary resource expansion plans. The introduction of wind and solar curtailment variables enhances the model's practical adaptability. Through iterative solving between the two levels, the model achieves organic integration between resource siting from the planning phase and dispatch strategies from the operational phase, significantly improving the economic efficiency of resource allocation while ensuring grid security.

Case studies based on a six-node system demonstrate that, compared to a singular configuration relying solely on energy storage, the synergistic "storage-load" configuration scheme activates the regulation potential of industrial loads. While satisfying the same flexibility requirements, it effectively reduces the scale of energy storage investment and the overall cost, and also decreases new energy curtailment losses. This validates the effectiveness of the proposed model in enhancing system economy and promoting new energy integration. This research not only provides an operational theoretical methodology and model support for the synergistic planning of flexible resources in urban power grids, but also fully demonstrates the significant engineering value of complementary coordination among diverse resources in strengthening grid resilience and driving the energy transition. It holds positive practical significance for guiding the planning and operation of urban power grids in the context of new-type power systems.

Acknowledgements.

This research has been funded by the Project Research on Wind-Solar-Storage (Vehicle-Load) Coordinated Configuration and Network Optimization Technology for Energy-Autonomous Rural Microgrids (5400-202324825A-4-1-KJ) supported by State Grid Corporation of China.

References

[1] Voropai N. Electric power system transformations: A review of main prospects and challenges[J]. Energies, 2020, 13(21): 5639.

[2] Bai F, Zhang K. The research progress on distributed generation and microgrid system stability: Progress, challenges, and frontier directions[J]. Advances in Resources Research, 2025, 5(4): 2366-2408.

[3] Ahmed M M R, Mirsaeidi S, Koondhar M A, et al. Mitigating uncertainty problems of renewable energy resources through efficient integration of hybrid solar PV/wind systems into power networks[J]. IEEe Access, 2024, 12: 30311-30328.

[4] Medina C, Ana C R M, González G. Transmission grids to foster high penetration of large-scale variable renewable energy sources–A review of challenges, problems, and solutions[J]. International Journal of Renewable Energy Research (IJRER), 2022, 12(1): 146-169.

[5] Yu S, Zhou S, Chen N. Multi-objective optimization of capacity and technology selection for provincial energy storage in China: The effects of peak-shifting and valley-filling[J]. Applied Energy, 2024, 355: 122289.

[6] Tan Y, Wen M, Liao J, et al. Scheduling strategy of energy storage peak-shaving and valley-filling considering the improvement target of peak-valley difference[C]//2021 11th International Conference on Power and Energy Systems (ICPES). IEEE, 2021: 196-200.

[7] Wang L Q, Liu H Q, Wang Q, et al. An intraday dispatch strategy for demand-side flexible resources based on two-stage optimization[J]. Frontiers in Energy Research, 2024, 12: 1343728.

[8] Li W S, Liang R, Luo F Z, et al. Response potential assessment of user-side flexible resources of regional power distribution networks based on sequential simulation of optimal operation[J]. Frontiers in Energy Research, 2022, 10: 1096046.

[9] Shao X S, Cui G Y, Chen X, et al. Optimal control strategy of platform load oriented to network and load cooperation[J]. Complexity, 2021, 2021: 9976473.

[10] Moghaddas-Tafreshi S M, Zamani H A, Hakimi S M. Optimal sizing of distributed resources in micro grid with loss of power supply probability technology by using breeding particle swarm optimization[J]. J. Renewable Sustainable Energy, 2011, 3(4): 043105.

[11] Han S. Research on interactive response strategy of power demand-side resources participating in power grid[C]//2020 International Symposium on Energy Environment and Green Development. 2021: 012109.

[12] Sun H D, Ren Y H, Wang S S, et al. Smart grid power load type forecasting: research on optimization methods of deep learning models[J]. Frontiers in Energy Research, 2023, 11: 1321459.

[13] DING Kun, ZHANG Lei, YANG Changhai, et al. The optimization analysis of multi-type demand-side flexibility resources for renewable energy accommodation in electrical power systems[J]. Frontiers in Energy Research, 2023, 11: 1333872.

[14] Crespi E, Guandalini G, Nieto Cantero G, et al. Dynamic modeling of a PEM fuel cell power plant for flexibility optimization and grid support[J]. Energies, 2022, 15(13): 4801.

[15] Zhang R, Yu J L. New urban power grid flexible load dispatching architecture and key technologies[J]. Frontiers in Energy Research, 2023, 11: 1168768.

[16] Lepszy S. Analysis of the storage capacity and charging and discharging power in energy storage systems based on historical data on the day-ahead energy market in Poland[J]. Energy, 2020, 213: 118815.

[17] Jiang H, Yao L, Zhang X, et al. Impact of spatial layout optimization on photovoltaic power consumption: insights from China[J]. International Journal of Digital Earth, 2025, 18(1): 2447339.

[18] Stanley A P J, King J. Optimizing the physical design and layout of a resilient wind, solar, and storage hybrid power plant[J]. Applied Energy, 2022, 317: 119139.

[19] Lara J D, Henriquez-Auba R, Ramasubramanian D, et al. Revisiting power systems time-domain simulation methods and models[J]. IEEE Transactions on Power systems, 2023, 39(2): 2421-2437.

[20] Xiao J W, Yang Y B, Cui S, et al. A new energy storage sharing framework with regard to both storage capacity and power capacity[J]. Applied Energy, 2022, 307: 118171.

[21] Yan X, Yu Y, Liu N, et al. Multi-service storage capacity management by cumulative prospect based portfolio theory[J]. CSEE Journal of Power and Energy Systems, 2023.